JOURNAL OF THE ROYAL SOCIETY Interface

The three-dimensional locomotor dynamics of African (*Loxodonta africana*) and Asian (*Elephas maximus*) elephants reveal a smooth gait transition at moderate speed

Lei Ren and John R Hutchinson

J. R. Soc. Interface 2008 **5**, 195-211
doi: 10.1098/rsif.2007.1095

JOURNAL OF THE ROYAL SOCIETY Interface

J. R. Soc. Interface (2008) **5**, 195–211
doi:10.1098/rsif.2007.1095

The three-dimensional locomotor dynamics of African (*Loxodonta africana*) and Asian (*Elephas maximus*) elephants reveal a smooth gait transition at moderate speed

Lei Ren* and John R. Hutchinson

Structure and Motion Laboratory, The Royal Veterinary College, University of London, Hawkshead Lane, North Mymms, Hatfield, Hertfordshire AL9 7TA, UK

We examined whether elephants shift to using bouncing (i.e. running) mechanics at any speed. To do this, we measured the three-dimensional centre of mass (CM) motions and torso rotations of African and Asian elephants using a novel multisensor method. Hundreds of continuous stride cycles were recorded in the field. African and Asian elephants moved very similarly. Near the mechanically and metabolically optimal speed (a Froude number (Fr) of 0.09), an inverted pendulum mechanism predominated. With increasing speed, the locomotor dynamics quickly but continuously became less like vaulting and more like bouncing. Our mechanical energy analysis of the CM suggests that at a surprisingly slow speed (approx. $2.2\ \mathrm{m\,s^{-1}}$, Fr 0.25), the hindlimbs exhibited bouncing, not vaulting, mechanics during weight support. We infer that a gait transition happens at this relatively slow speed: elephants begin using their compliant hindlimbs like pogo sticks to some extent to drive the body, bouncing over their relatively stiff, vaulting forelimbs. Hence, they are not as rigid limbed as typically characterized for graviportal animals, and use regular walking as well as at least one form of running gait.

Keywords: elephant; Proboscidea; locomotion; biomechanics; dynamics; gait

1. INTRODUCTION

As the epitome of graviportal animals (Gregory 1912; Gray 1968; Coombs 1978), elephants possess pillar-like legs for supporting their massive body weight (exceeding 7000 kg in some animals; Wood 1972; Christiansen 2004). Even at moderately fast speeds, elephants hold their legs relatively straight when on the ground, with estimated strain levels in lower leg bones similar to those of much smaller running animals (Alexander 1977; Alexander *et al.* 1979; Rubin & Lanyon 1984; Biewener & Taylor 1986). But do these fairly straight, although not necessarily completely columnar, limbs obviate the ability to use the limbs in a compliant, bouncing fashion? Elephants are a superb model system to gain insight into how musculoskeletal design is a compromise with the biomechanical and physiological constraints that extremely large body size imposes, and to test if, when, how and why locomotor abilities become lost at large size. Here we develop a new inertial sensor-based method to estimate the rigidness/compliance of elephant limbs, by quantifying centre of mass (CM) motions in locomotion, which are key indicators of limb/body compliance (Farley *et al.* 1993; Biknevicius *et al.* 2006).

Elephants are unusual not only in their enormous size, but also in their special locomotor pattern (Hutchinson *et al.* 2003, 2006). Elephants do not normally trot or gallop, even as juveniles, but they can move smoothly to fairly fast speeds (approx. $6.8\ \mathrm{m\,s^{-1}}$) without changing their lateral sequence footfall pattern (Hutchinson *et al.* 2003). Their locomotor pattern at their faster speeds is atypical of most familiar quadrupedal animals (Muybridge 1899; Gambaryan 1974; Hildebrand 1985). Fast moving elephants exceed Froude numbers (Fr, where $\mathrm{Fr}=\mathrm{velocity}^2\times(\text{gravitational acceleration}\times\text{hip height})^{-1}$) of 1.0, even reaching Fr 3.4 (Hutchinson *et al.* 2003), speeds at which most other quadrupedal mammals gallop (Alexander & Jayes 1983). Across their entire speed range, elephants constantly keep at least one foot on the ground; they never change their footfall pattern to one that uses a whole-body aerial phase (Hutchinson *et al.* 2003, 2006).

The kinematics of slow moving elephants fall nicely into the definition of walking from all aspects, but fast moving elephants pose a challenge for applying many gait definitions. This issue hinges on how one defines a gait

---

*Author for correspondence (lren@rvc.ac.uk).

Electronic supplementary material is available at http://dx.doi.org/10.1098/rsif.2007.1095 or via http://journals.royalsociety.org.

Received 7 May 2007
Accepted 31 May 2007

Table 1. Vital data for elephants used in this study. (Woburn: Woburn Safari Park, Bedfordshire, UK; WMSP: West Midlands Safari Park, West Midlands, UK. 'Shoulder' height was measured from the top of the scapula, not the glenohumeral joint, as typical for elephant studies.)

elephant	facility	species	sex	age (years)	weight (kg)	hip height (m)	shoulder height (m)
Chandrika	Woburn	Asian	F	14	3000	1.97	2.46
Damini	Woburn	Asian	F	12	2840	2.08	2.42
Five	WMSP	African	F	14	2780	2.06	2.47
Jack	WMSP	African	M	13	3230	2.03	2.59
Latabe	WMSP	African	F	13	2550	1.84	2.41

(see §4 here and in Hutchinson *et al.* 2006). For most animals, the kinematic (e.g. aerial phase) and kinetic (i.e. shift from vaulting to bouncing mechanics, e.g. Biewener 2006; Biknevicius & Reilly 2006) definitions normally lead to the same conclusion. However, when applied to the fast moving elephants, they are partly contradictory (Hutchinson *et al.* 2006). Previous studies doubted whether fast moving elephants were merely walking (Hutchinson *et al.* 2003), but the speed at which any potential gait transition occurred was left open, although it was concluded that near a dimensionless speed of 1.0 (equal to $Fr^{0.5}$, 1.0) elephants probably were running, in the mechanical sense of the term.

It is generally accepted that at least two fundamental mechanisms are employed by animals to modulate their energy costs in terrestrial locomotion (Cavagna *et al.* 1977; Heglund *et al.* 1982*a*,*b*; McGeer 1992; Farley *et al.* 1993; Minetti 2000; Ruina *et al.* 2005). Inverted pendulum-like movement of the body's CM during slower locomotion is characterized by exchange of potential and kinetic energies associated with conservation of mechanical energy via a vaulting mechanism (Cavagna *et al.* 1977; McGeer 1992; Biewener 2006; Biknevicius & Reilly 2006). During running, trotting, hopping or Groucho (compliant) walking/running, kinetic and potential energies fluctuate in phase, but energy is conserved to some extent as the body bounces on somewhat elastic legs (Cavagna *et al.* 1977; McMahon *et al.* 1987; Farley *et al.* 1993). Despite their massive body weights and ponderous motions, elephants are the most economical living land animals, moving very cheaply at their normal walking speed in terms of metabolic cost of transport ($\mathrm{J\,kg^{-1}m^{-1}}$; African elephant data from Langman *et al.* 1995). Hence, some energy-saving mechanism (very likely pendulum-like walking; although elastic mechanisms may contribute even in walking, e.g. Geyer *et al.* 2006) must be utilized by elephants at their energetically optimal speed. However, as speed increases, elephants should change their locomotor pattern at least in a biomechanical sense, as inverted pendulum-like walking (i.e. vaulting) becomes more and more expensive in terms of metabolic cost (Hoyt & Taylor 1981; Farley & Taylor 1991), and even impossible at faster speeds (Usherwood 2005). Although basic information on footfall patterns and other stride parameters are now available, providing hints that a bouncing gait (i.e. running in a biomechanical sense; Cavagna *et al.* 1977; Farley *et al.* 1993; Ruina *et al.* 2005) may be used at moderate to near-maximal speeds (Hutchinson *et al.* 2003, 2006), there are still wide gaps in the fundamental understanding of elephant locomotion.

The major objective of this study is to quantify the three-dimensional locomotor dynamics of Asian (*Elephas maximus* Linnaeus 1758) and African (*Loxodonta africana* Blumenbach 1797) elephants. We aim to test whether bouncing limb or CM mechanics are used at any speed (i.e. do elephants run?), or if all observable speeds in elephants comprise only standard vaulting mechanics (do they only walk?). Here we separate limb and CM mechanics, as the possibility remains that elephant limbs do not function identically (Hutchinson *et al.* 2006) and at some speeds vaulting whole-body CM mechanics still could involve spring-like functioning of some limbs. We also sought to identify whether there were any major kinetic differences between Asian and African elephants, as their kinematics are very similar (Hutchinson *et al.* 2006) but it is not impossible that there would be underlying kinetic differences.

We developed a novel multiple inertial sensor method, following Pfau *et al.* (2005, 2006), incorporating three-dimensional accelerometers and gyroscopes to measure the three-dimensional body CM dynamics and the torso rotations of several elephants (here we use the term 'torso' to refer to the limbless body, rather than 'trunk', which in the case of elephants may confuse readers, or 'body', which we only use to refer to the whole body with all four limbs included). Hundreds of continuous strides were recorded as the elephants moved freely outside in open fields at a range of speeds (0.5–$3.5\ \mathrm{m\,s^{-1}}$). We calculated the three-dimensional CM velocities and vertical displacements in each stride and we determined the potential energy, translational and rotational kinetic energies at different speeds. We also investigated the mechanical energy transductions in all the strides, and examined the possible gait pattern changes across the speed range.

2. METHODS

2.1. Animal measurements

Five healthy adult elephants were used in this study: two Asian elephants from Woburn Safari Park (Bedfordshire, UK) and three African elephants from West Midlands Safari Park (West Midlands, UK). Prior to testing, we used flexible measuring tape to record elephant hip and shoulder heights, and hip–hip, shoulder–shoulder and hip–shoulder distances. All elephants had known body masses (m_b) from placing all four limbs on a truck scale (± 2 kg). The vital data for each elephant used in this study are listed in table 1.

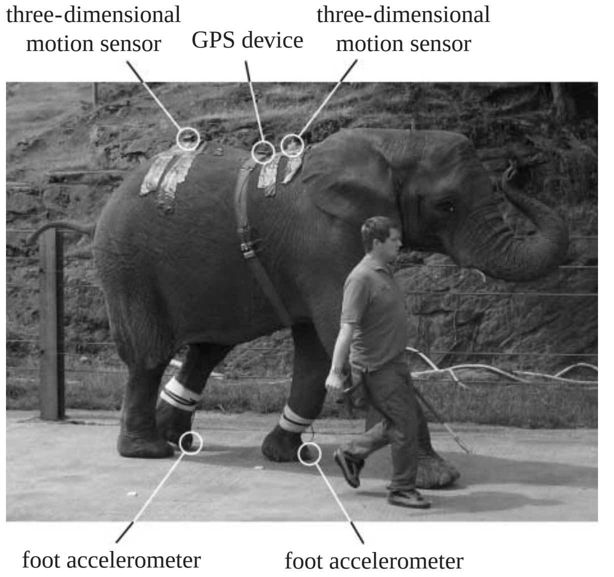

Figure 1. An African elephant moving with body-mounted sensor devices.

Each elephant was equipped with two miniature integrated inertial sensors (MT9, Xsens, Enschede, Netherlands), two foot-mounted accelerometers (ADXL150, Analogue Devices, Norwood, MA, USA), and one stand-alone Global Positioning System (GPS) device (BTGPS II, EMTAC Technology, USA; figure 1). Each inertial sensor unit, incorporating a three-dimensional accelerometer, a three-dimensional gyroscope and three magnetometers, provided three-dimensional translational accelerations, rates of gyration and orientation data for their point of attachment to the torso (Xsens, Enschede, Netherlands). The two inertial sensors were mounted on specially designed attachment pads and firmly attached to the elephant's torso, with one over the spinous processes of the thoracic vertebrae on the caudal border of the scapula, and the other over the spinous processes of the caudalmost lumbar vertebrae just on the dorsal peak of the hindquarters. The sensor data were recorded at a sample rate of 256 Hz and transmitted to two data loggers (Anticyclone Systems, Surrey, UK), which were mounted on the elephant using an elastic strap around the mid-torso. The GPS unit was mounted securely on the dorsal peak of the torso strap, and recorded 1 Hz data of heading speed, latitudinal and longitudinal position and universal time.

Prior to the trials, an inertial sensor was located on the ground surface, aligned with the trackway to record a trackway coordinate system (figure 2). Thereafter, the inertial sensors and foot accelerometers were synchronized at the beginning of the trials, and the universal time was recorded simultaneously to allow synchronization of the GPS data with the inertial sensor data.

Foot touchdowns and lift-offs for the two right limbs were determined by measuring foot acceleration using two uni-axis accelerometers (ADXL150, Analogue Devices, Norwood, MA, USA; Witte *et al.* 2004). The accelerometers were mounted on the dorsal side of the toenail of each middle toe using melted glue, with their sensitive axis along the proximal–distal direction. The signals were logged to two data loggers (customized MP3 recorders) and recorded at a sample rate of 44.1 kHz (Parsons & Wilson 2006). Each data logger was mounted on the lateral aspect of the distal ulna/fibula on the right limbs using elastic bandages.

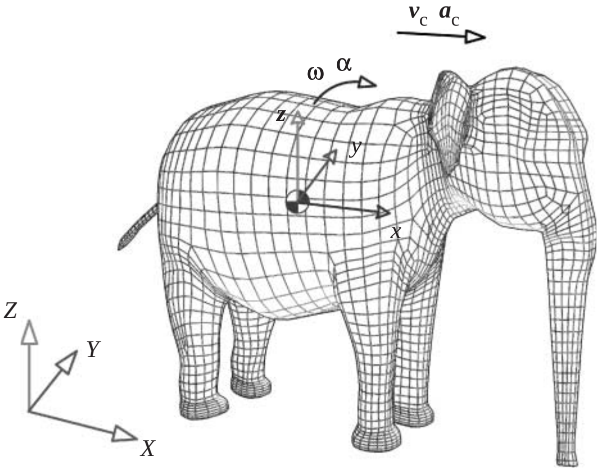

Figure 2. Two coordinate systems used to track elephant motions. A trackway coordinate system XYZ was defined by aligning the axes with the trackway. A body-fixed coordinate system xyz was defined to move with the elephant body. The derived CM velocity $\boldsymbol{v}_\mathrm{c}$ and acceleration a_c, and torso angular velocity $\boldsymbol{\omega}$ and angular acceleration $\boldsymbol{\alpha}$ were all expressed in the body-fixed coordinate system.

The elephants moved along level trackways of approximately 30 m (Woburn Safari Park) and approximately 25 m (West Midlands Safari Park) lengths at various speeds. This allowed the animals to accelerate or decelerate to and from even their fastest speeds. They were led by trainers in most trials (no difference was seen between led and not led). At fast speeds, they were also motivated by food rewards and trainer's requests. The sensors and recording system are lightweight and completely body mounted, so the elephants moved untethered and negligibly weighted. No behavioural artefacts were observed in how the elephants moved at any particular speed. The entire trial period normally lasted approximately 70 min, and the entire range of speed of the elephants was covered. Inertial sensor, foot accelerometer and GPS data were collected continuously. A total of 153 trials were recorded: 42 for Asian elephants (Woburn Safari Park) and 111 for African elephants (West Midlands Safari Park).

2.2. Multiple sensor method

It was previously demonstrated that using just one of the inertial sensors, the three-dimensional displacement of a horse's body CM can be captured with accuracy comparable to optical motion capture systems (Qualisys AB, Savedalen, Sweden) during trotting at up to 9.0 m s^{-1} (Pfau *et al.* 2005). In this study, we use an improved new sensor method to estimate the body CM acceleration, by combining the data from multiple inertial sensors attached at different positions of the animal body, similar to Hayes *et al.* (1983) and van den

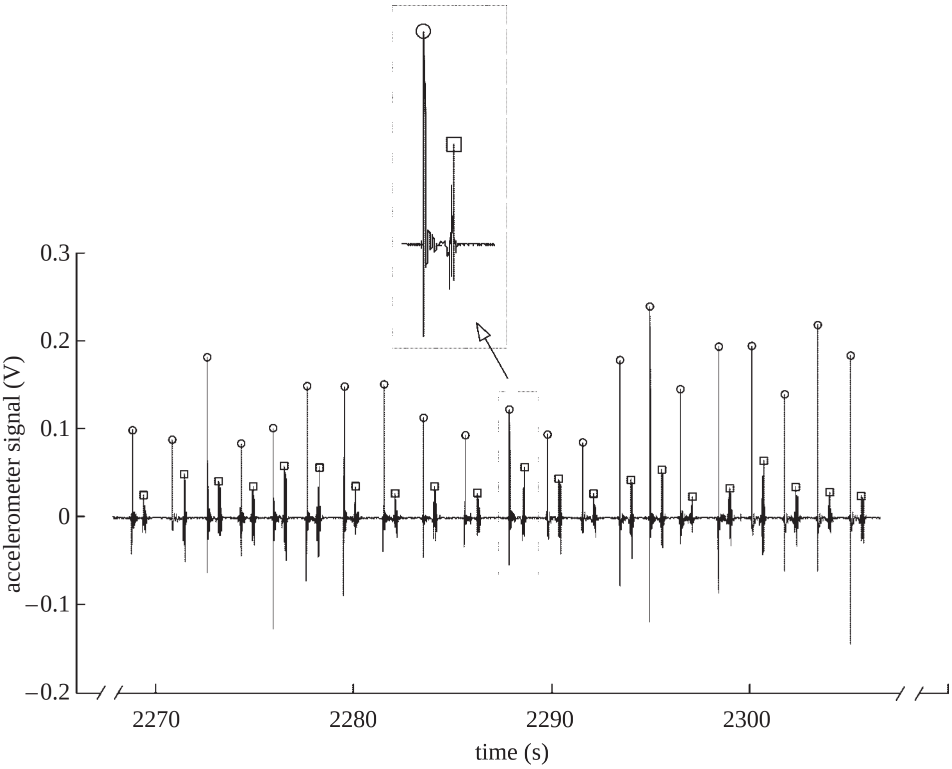

Figure 3. A trace of foot accelerometer signal with determined touchdowns (open squares) and lift-offs (open circles) for the right forelimb of an African elephant walking at approximately 1.3 m s^{-1}.

Bogert *et al.* (1996). A major advantage of using multiple sensors is that it provides an optimal estimation of the body CM acceleration by combining the motion data of different parts of the body, rather than only one particular part (Morris 1973; Hayes *et al.* 1983; van den Bogert *et al.* 1996). As the fore and hindquarters move differently in walking due to the limb phase differences, the body CM motion is a combination of both fore and hindquarter motions (Griffin *et al.* 2004*a*). Therefore, a multiple sensor method using both fore and hindquarter sensors is more suitable in this study.

In addition to an earth-fixed and sensor-fixed coordinate system inherently defined in the inertial sensors (Xsens, Enschede, Netherlands), a local (body-fixed) coordinate system fixed on the animal body was defined (figure 2). The origin lay at the whole-body CM of the animal, with the x-axis pointing in the horizontal (cranial) direction, the y-axis pointing left and the z-axis pointing dorsally. When an inertial sensor is attached to the animal at a known position $\boldsymbol{r}$ with respect to the body CM (the position of the inertial sensor relative to the body CM was determined using a three-dimensional geometric elephant model and the measured dimensional data; see details below), it generates the following linear acceleration vector (in the sensor-fixed coordinate system),

$$\boldsymbol{a} = \boldsymbol{a}_{\mathrm{c}} + \boldsymbol{g} + \boldsymbol{\omega} \times (\boldsymbol{\omega} \times \boldsymbol{r}) + \boldsymbol{\alpha} \times \boldsymbol{r}, \qquad (2.1)$$

where $\boldsymbol{a}_{\mathrm{c}}$ is the translational acceleration vector of the animal's body CM; $\boldsymbol{g}$ is the gravitational acceleration vector; $\boldsymbol{\omega}$ is the angular velocity vector measured by the gyroscopes expressed in the sensor-fixed coordinate system; and $\boldsymbol{\alpha}$ is the angular acceleration vector. When signals from n inertial sensors attached to the animal body are recorded, n of these equations lead to a linear simultaneous equation with two unknown kinematic variables ($\boldsymbol{a}_{\mathrm{c}}, \boldsymbol{\alpha}$). The Moore–Penrose pseudoinverse method (Campbell & Meyer 1991) was used to solve the equation. When the system is overdetermined ($n > 2$), the redundancy of the inertial sensor is used to improve the accuracy. The calculation was initially conducted in a sensor-fixed coordinate system, and finally the derived results ($\boldsymbol{a}_{\mathrm{c}}, \boldsymbol{\alpha}$) were converted into the body-fixed coordinate system of the animal. In contrast to multiple sensor methods using only accelerometer data (Kane *et al.* 1974; Hayes *et al.* 1983; van den Bogert *et al.* 1996), which need iterative runs of nonlinear solvers and a good initial guess, this method provides a linear closed-loop solution to estimate the whole-body CM acceleration without requiring differentiation and integration.

2.3. Data analysis

GPS data were downloaded from the GPS device using CRUX II GPS software (EMTAC Technology, USA). Speed data were extracted for each second using custom software in MATLAB (Mathworks, Natick, MA, USA). The foot accelerometer data were also processed using custom MATLAB software. The data were first resampled to the sample rate of the inertial sensors, and then the foot touchdown and lift-off timings were identified manually based on the accelerometer signals (Witte *et al.* 2004). Figure 3 shows a trace of resampled foot accelerometer signal with determined touchdowns and lift-offs for the right forelimb of an African elephant walking at approximately 1.3 m s^{-1} (in contrast to horses (Witte *et al.* 2004), the touchdown peak signal of elephants is much lower than that of lift-off, presumably due to their large, soft foot pads). The GPS data were synchronized with the accelerometer data based on the universal time recorded. We averaged the GPS speed data within each gait cycle to calculate the average locomotor speed of that stride based on foot-on and foot-off timings.

Our multiple sensor method was implemented in Matlab (Mathworks, Natick, MA, USA) to process the inertial sensor data. The sensor signal data first were segmented into each stride based on the touchdown and lift-off events determined from the foot accelerometer data. Next, the data were filtered using a low-pass, zero-lag fourth-order Butterworth digital filter with a cut-off frequency of 10 Hz. The body-fixed coordinate systems of the elephants were defined for each stride based on the average progression direction in the stride and the vertical axis of the trackway coordinate system. Thereafter, the multiple sensor algorithm was used to derive the three-dimensional body CM accelerations and angular accelerations from the filtered signal data of the two inertial sensors. The calculation was initially conducted in the sensor-fixed coordinate system of the forequarters' inertial sensor, and finally the derived results were converted into the body-fixed coordinate system of the elephants. The linear acceleration and heading direction data were examined stride by stride, and all accelerating, decelerating and turning strides were discarded. We used the averaged horizontal acceleration in a stride to identify acceleration and deceleration cycles. A threshold of ±10% of peak horizontal acceleration was used to discard the accelerating and decelerating cycles. The heading direction recorded by the magnetometers on the forequarters was used to find straight moving strides, where a threshold of ±20° was used.

In the multiple sensor algorithm, knowledge of the whole-body CM position of the elephants is required to determine the relative position of each inertial sensor. However, there are no empirical body CM position data for elephants based on direct cadaver measurements. In this study, the body CM positions were determined based on a three-dimensional geometric elephant model (including all four limbs and other appendages) using validated three-dimensional graphics software (figure 4), which uses interactive deformable B-spline solids to estimate the inertial parameters for animal body segments (Hutchinson *et al.* 2007). The initial three-dimensional model was originally constructed based on an Asian elephant (based on a graphical artist's representation). For each elephant, the body size and shape of the model was scaled in different directions according to the dimensional values measured for the individual elephants (hip and shoulder heights, hip–hip, shoulder–shoulder and hip–shoulder lengths), and sculpted to conform well to photos of the individuals (including minor differences in Asian versus African elephant body shape). The body mass, body CM position and inertial tensor around the CM (J_c) were calculated using isotropic material with a density of 1000 kg m^{-3}. The inertial product components were very small, and hence were neglected. Therefore, the three principal axes of the inertia tensor coincided with the axes of the animal body-fixed coordinate system, and the inertial tensors were defined by three principal components (I_{xx}, I_{yy}, I_{zz}). Table 2 lists the inertial parameters for each elephant. We found the inertial sensor positions with respect to the body CM by moving a reference point interactively in the three-dimensional software environment, and simultaneously referring to multiple photos (taken from different views) of standing elephants mounted with sensors in the trials.

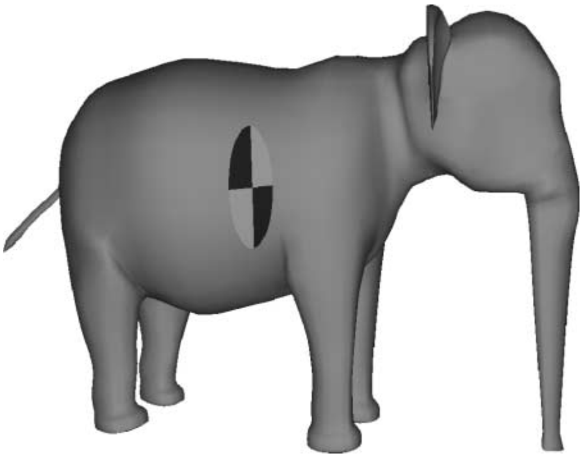

Figure 4. A three-dimensional geometric elephant (in right lateral view) used to estimate the inertial parameters for elephants.

Energy analysis was conducted in each stride to assess the mechanical energy fluctuations, mechanical work and power required to move the CM and rotate the animal's body (Cavagna & Kaneko 1977; Cavagna *et al.* 1977). Total mechanical energy E_m comprises two components: potential energy $E_p = m_b g z_c$ and kinetic energy $E_k = E_{kt} + E_{kr}$, where z_c is the vertical position of the body CM and E_{kt} and E_{kr} are the translational and rotational kinetic energies, respectively, defined as $E_{kt} = (1/2) m_b \boldsymbol{v}_c \cdot \boldsymbol{v}_c$ and $E_{kr} = (1/2) \boldsymbol{\omega} \cdot (J_c \cdot \boldsymbol{\omega})$. CM acceleration data were numerically integrated to calculate the CM velocity $\boldsymbol{v}_c$. The average locomotor speed in a stride was used as the integration constant for horizontal speed, and the average vertical and lateral speeds were assumed as zero. The derived vertical velocity was then integrated to calculate the vertical displacement of the CM, z_c, using zero as the integration constant. The total mechanical power provided by the limbs to maintain the energy fluctuations of the elephant's body was defined as the time derivative of the total mechanical energy $P_m = (\mathrm{d}E_m/\mathrm{d}t)$. Like E_m, it is the instantaneous sum of two terms, $P_p = (\mathrm{d}E_p/\mathrm{d}t)$ and $P_k = (\mathrm{d}E_k/\mathrm{d}t)$, defined as $P_p = m_b g \dot{z}_c$ and $P_k = m_b \boldsymbol{v}_c \cdot \boldsymbol{a}_c + (\boldsymbol{\alpha} \cdot (J_c \cdot \boldsymbol{\omega}) + \boldsymbol{\omega} \cdot (J_c \cdot \boldsymbol{\alpha}))/2$.

To quantitatively estimate the theoretical energy saving due to the transfer between potential and kinetic energies for inverted pendulum-like walking, percentage energy recovery was calculated in each stride as (Cavagna *et al.* 1977; Heglund *et al.* 1982*a*,*b*)

$$C_s = \frac{\Delta E_p + \Delta E_k - \Delta E_m}{\Delta E_p + \Delta E_k}, \qquad (2.2)$$

where ΔE_p is the sum of the positive increment of E_p; ΔE_k is the sum of the positive increment of E_k; and ΔE_m

Table 2. Estimated inertial parameters for elephants used in this study. (I_{xx}, I_{yy}, I_{zz}: three principal components of whole-body inertial moment around the CM.)

elephant	measured mass (kg)	estimated mass (kg)	estimation error (%)	I_{xx} (kg m^2)	I_{yy} (kg m^2)	I_{zz} (kg m^2)
Chandrika	3000	3033	1.1	796.0	2232	1888
Damini	2840	2859	0.70	721.3	2022	1711
Five	2780	2817	1.3	703.6	1973	1669
Jack	3230	3260	0.90	897.9	2517	2130
Latabe	2550	2415	5.3	544.4	1526	1291

is the sum of the positive changes in total mechanical energy E_m (the rotational kinetic energy E_kr was removed from E_m when calculating the energy recovery). The phase shift angle between the potential and kinetic energies of the CM (representing how far out of phase they are) was also calculated for each stride, with 180° being totally out of phase (i.e. ideal vaulting) and 0° being exactly in phase (i.e. ideal bouncing). If there were two small kinetic energy peaks in a step (typical for slower motion), the midway point of the two peaks was used to define the phase angle, by representing the general phase relationship between the kinetic and potential energy fluctuations (similar results were obtained using the minimum kinetic energy and maximum potential energy as in Griffin *et al.* 2004*a*). The relative magnitude of the kinetic energy fluctuation with respect to the potential energy fluctuation was also calculated.

3. RESULTS

We collected 876 strides of valid data for the 153 trials and show representative time trace curves of an African elephant moving at 1.37 (figure 5) and 3.07 m s^{-1} (figure 6). We confirmed that all representative traces shown were broadly consistent among trials and individuals. Both horizontal (a_x) and lateral (a_y) CM accelerations fluctuated around zero. The horizontal acceleration exhibited a typical sinusoidal pattern at all speeds in each step. The lateral component was of small amplitude and greater variability than the other directions, especially during faster locomotion. The vertical CM acceleration a_z fluctuated around gravitational acceleration (9.8 m s^{-2}) with two or three small peaks in each step. The fluctuation amplitude of vertical acceleration was approximately 3 m s^{-2} at 1.37 m s^{-1}, and increased only moderately to 7 m s^{-2} at 3.07 m s^{-1}. Both the horizontal and vertical CM accelerations at slow speeds broadly matched previous force plate and modelling data for slowly walking dogs and other quadrupeds (Cavagna *et al.* 1977; Griffin *et al.* 2004*a*; Usherwood *et al.* 2007). The torso angular velocities (roll ω_x, yaw or heading ω_z and pitch ω_y) all oscillated cyclically around zero with small amplitude, and increased only slightly when speed increased to 3.07 m s^{-1}. Similar to angular velocity, the angular accelerations (α_x, α_y, α_z) also fluctuated periodically around zero in each stride. However, they increased markedly when speed increased.

Representative averaged curves of translational kinetic energy (E_kt), total kinetic energy ($E_\mathrm{kt}+E_\mathrm{kr}$), potential energy ($E_\mathrm{p}$) and mechanical energy (E_m) of an African elephant moving at 1.37 and 3.07 m s^{-1} are shown in figures 7 and 8 (corresponding to figures 5 and 6). At slower speeds, the rotational kinetic energy (E_kr) due to torso rotations only accounted for very small amount of the total kinetic energy, even at moderate speed (3.07 m s^{-1}). Although the inertia tensors of elephants are very large due to the massive body mass and size, the torso angular velocities were relatively small. The total kinetic energy showed a two-peaked pattern per stride, reaching its minima in the forelimb mid-stance phase and its maxima in the forelimb double support phase. The potential energy also showed a two-peaked pattern that was almost out of phase with kinetic energy, reaching minima around forelimb touchdown and maxima between mid-stance of the supporting hindlimb and mid-stance of the supporting forelimb. These potential and kinetic energy patterns in a stride closely match the trends from previous force plate and modelling data for walking dogs and other quadrupeds at slow and normal speeds (Cavagna *et al.* 1977; Griffin *et al.* 2004*a*; Usherwood *et al.* 2007). Although the mechanical energy fluctuations were small throughout most of the stride, there were still some distinct mechanical energy changes (energy inputs and losses), especially as the CM raised towards its highest position.

When speed increased to 3.07 m s^{-1} (figure 8), the potential energy showed a similar pattern to slow speeds, but its greatest magnitude shifted closer to the timing of the contralateral hindlimb touchdown. The total kinetic energy increased markedly due to the speed increase, and was dominated by translational kinetic energy. In contrast to the 2.24 times slower speed shown, the relative magnitude of the kinetic energy with respect to potential energy increased more than three times, from 126 to 410%. However, unlike at slower speeds, the kinetic energy became more in-phase with potential energy at faster speeds, reaching its maxima shortly after the lift-off of each forelimb, during the late stance phase of the contralateral hindlimb.

The estimated vertical CM displacements (figure 9; corresponding to figures 7 and 8) had very similar patterns at slower and faster speeds, showing two peaks in a stride. There were no striking changes in the fluctuation amplitude of the vertical CM displacements when speed increased from 1.37 to 3.07 m s^{-1}; the fluctuation ranges were approximately 30 mm in both cases. However, as was the case for potential energy, the timing of the maximum vertical displacement moved towards the contralateral hindlimb touchdown when speed increased.

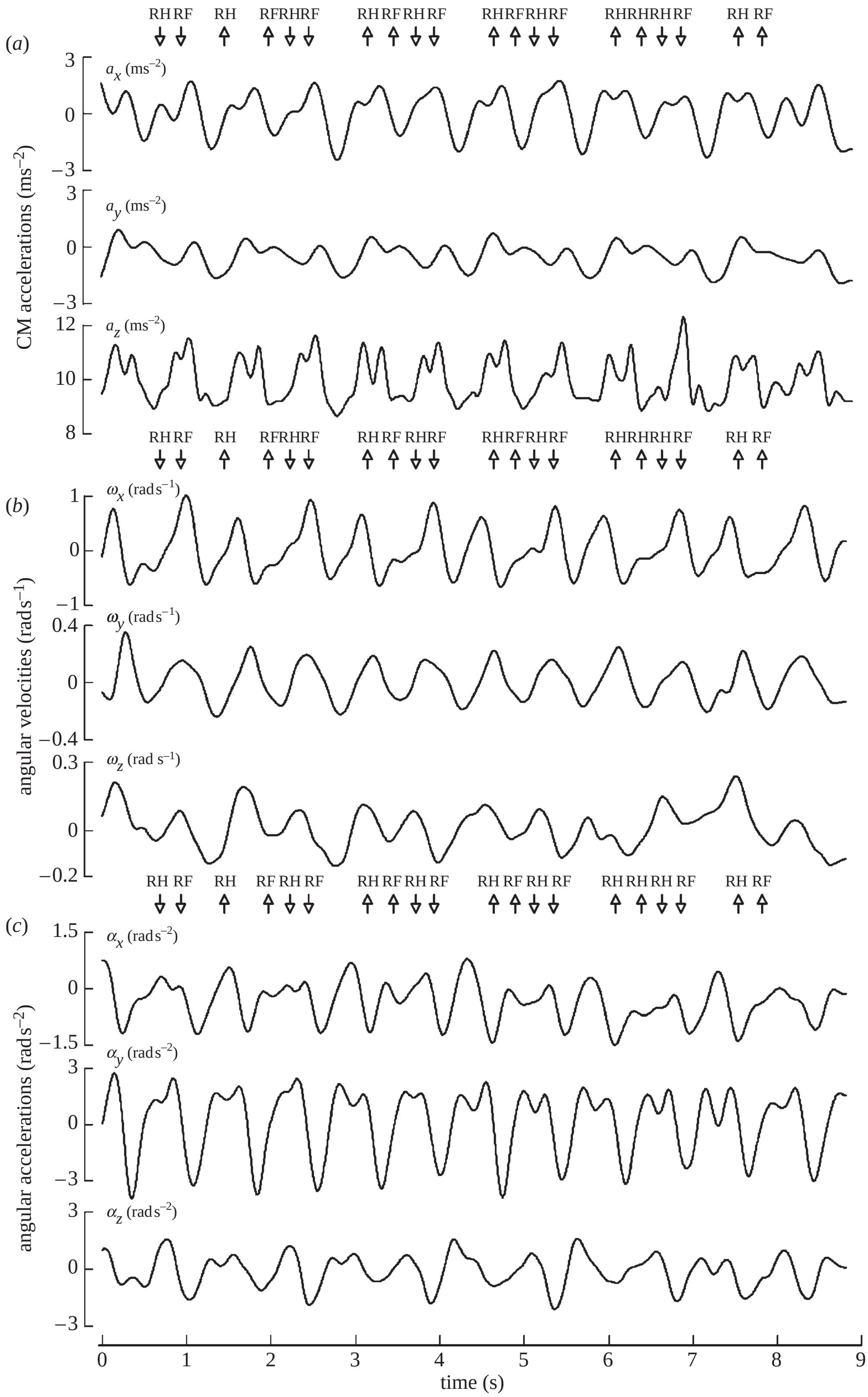

Figure 5. Representative time traces of (*a*) three-dimensional CM accelerations, (*b*) torso angular velocities and (*c*) angular accelerations of an African elephant (2780 kg) moving at 1.37 m s^{-1}, with approximately 4.5 continuous steady strides. RH and RF (above) show foot touchdown and lift-off events from the accelerometer data.

At slower speeds, the total CM mechanical power was of small amplitude (figure 9). The elephants used alternating periods of double and triple limb support at the speeds shown. During the early part of triple limb support (just after a hindlimb touchdown, when both hindlimbs and the contralateral forelimb were on the ground), the mechanical power exhibited only very small fluctuations. This is consistent with the inference that an inverted pendulum mechanism is very effective during this period in elephants. Just before each forelimb's touchdown, there was a burst of positive power, presumably to reduce the touchdown collisional losses

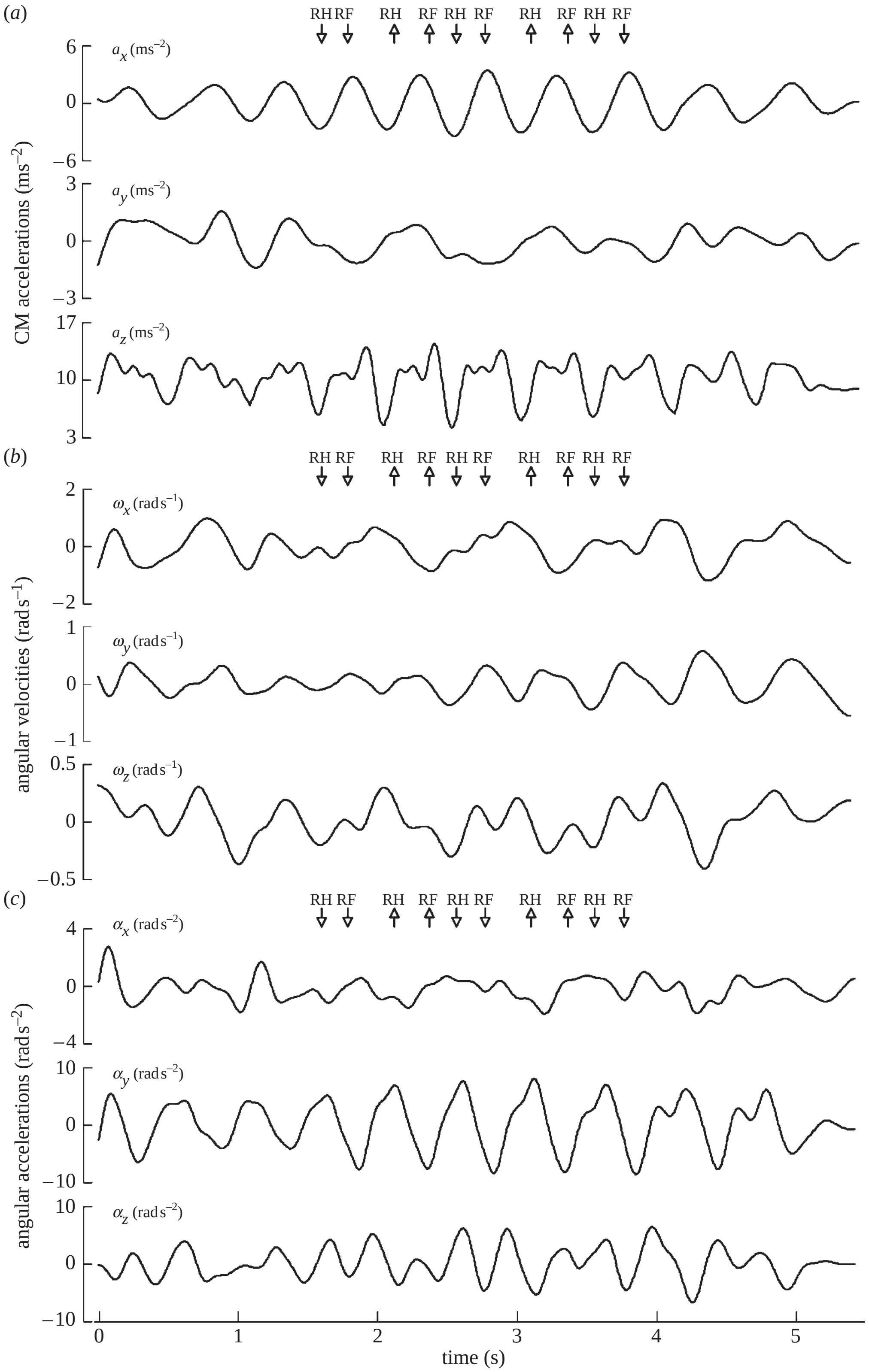

Figure 6. Representative time traces of (*a*) three-dimensional CM accelerations, (*b*) torso angular velocities and (*c*) angular accelerations of an African elephant (2780 kg) moving at 3.07 m s^{-1}, with approximately 2.5 continuous steady strides.

and hence save energy (Kuo 2002; Ruina *et al.* 2005; Usherwood *et al.* 2007). This positive power continued until slightly before the next forelimb lift-off, raising the elephant's CM to its highest position presumably via the trailing forelimb's push-off. Thereafter, the mechanical power became slightly negative, probably due to the simultaneous positive and negative work of the ipsilateral forelimb and hindlimb (Donelan *et al.* 2002). After the contralateral hindlimb landed on the ground, the animal passed into its next triple support phase.

At faster speeds, the pattern of CM mechanical power totally changed, even though the footfall pattern remained almost identical. This change was not sudden, but was rather continuous across the range of speeds

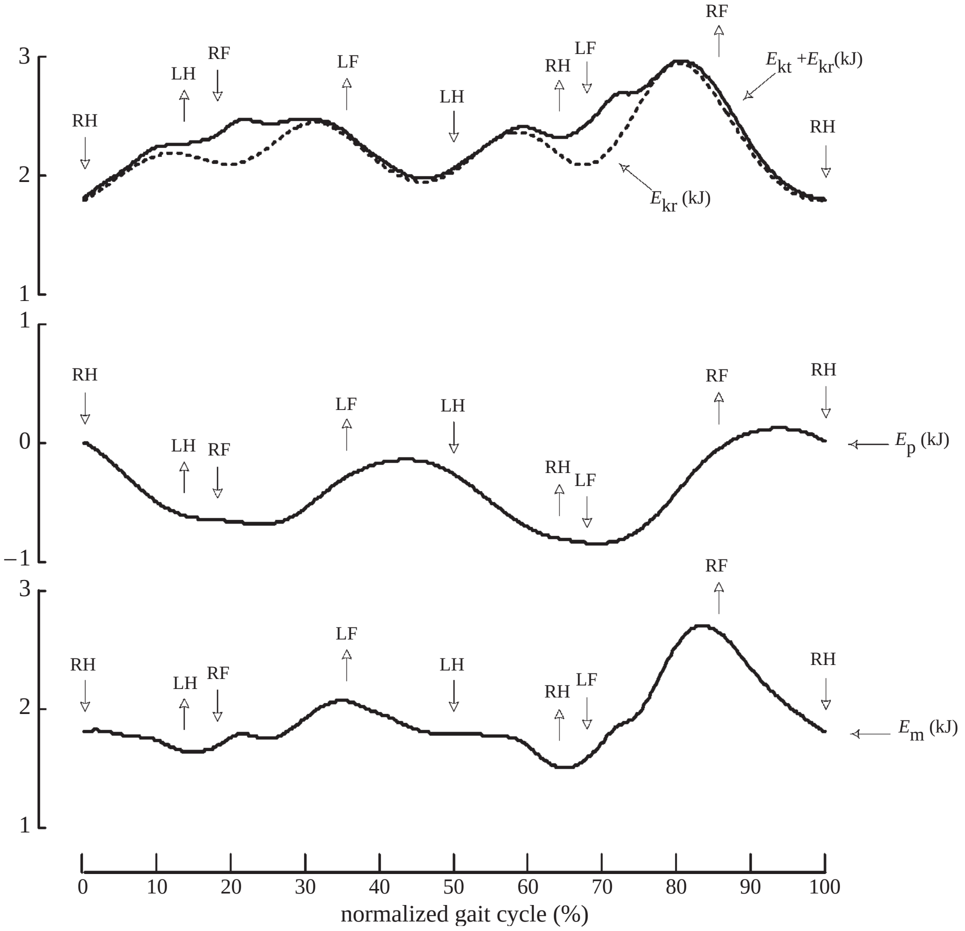

Figure 7. Representative time histories of translational kinetic energy E_{kt}, total kinetic energy $E_{kt}+E_{kr}$, potential energy E_p and total mechanical energy E_m in a stride cycle of an African elephant (2780 kg) moving at 1.37 m s^{-1} (Fr 0.093), averaged for four continuous strides (corresponding to figure 4). Left limb touchdowns and lift-offs were estimated by assuming a half stride phase difference between right and left limbs (Hutchinson *et al.* 2006).

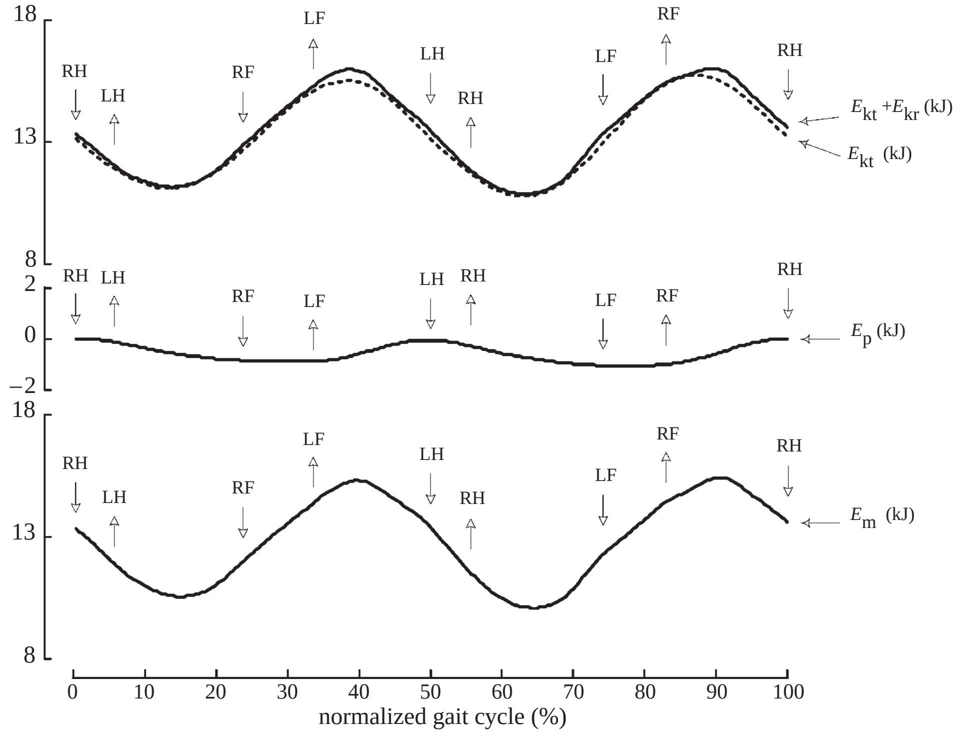

Figure 8. Representative time histories of translational kinetic energy E_{kt}, total kinetic energy $E_{kt}+E_{kr}$, potential energy E_p and total mechanical energy E_m in a stride cycle of an African elephant (2780 kg) moving at 3.07 m s^{-1} (Fr 0.47), averaged for two continuous strides (corresponding to figure 5).

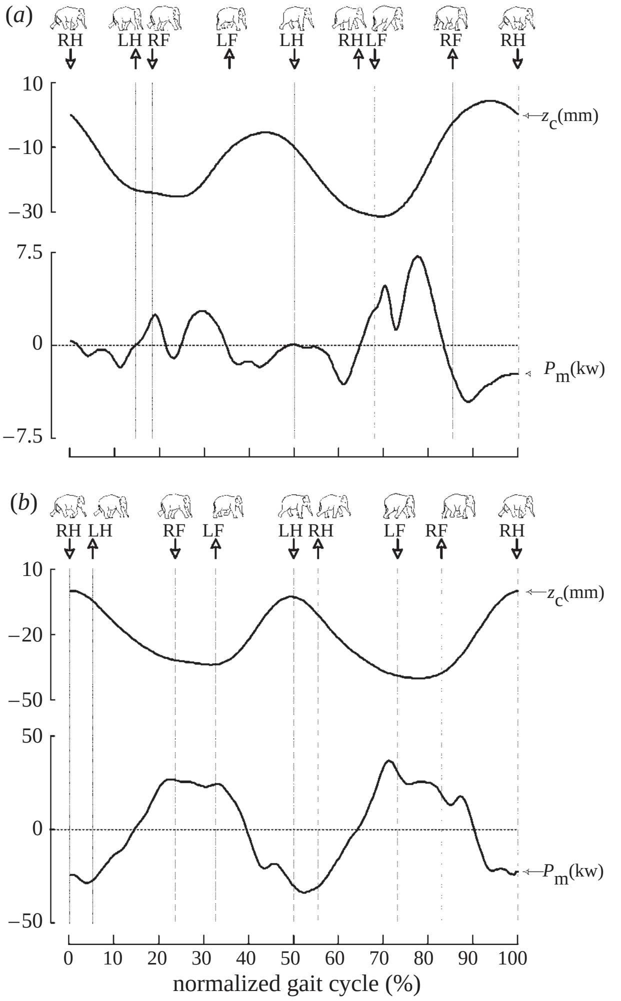

Figure 9. Representative averaged time histories of vertical CM displacement and total mechanical power in a stride cycle of an African elephant (2780 kg) moving at (*a*) 1.37 m s^{-1} (Fr 0.093) and (*b*) 3.07 m s^{-1} (Fr 0.47) (corresponding to figures 4 and 5). Elephant pictures modified from Gambaryan (1974).

observed. There were two large negative power bursts and two large positive bursts per stride. The mechanical energy losses occurred in early hindlimb stance and were recovered near the hindlimb mid-stance phases. In contrast to slower speeds, the positive power burst continued after the contralateral forelimb left the ground, when only the ipsilateral forelimb and hindlimb were in stance.

Very similar to the African elephants described above, the total kinetic energy and potential energy of Asian elephants (figures 10 and 11) during a stride were also almost out of phase at around their metabolically optimal speed, with phase shift angles approximately 145°–165°, very close to the 150°–170° of African elephants (figures 7 and 8). When speed increased to 2.41 m s^{-1}, this phase relationship changed to more in-phase. The vertical CM displacement also showed a two-peaked pattern at both speeds, with its maximum position being between mid-stance of the supporting hindlimb and mid-stance of the supporting forelimb at slower speeds, and moving towards the contralateral hindlimb touchdown when speed increased. It showed no particular change in its fluctuation amplitude with increasing speed, which was approximately 28–35 mm, very similar to 30–38 mm of African elephants (figure 9). The total mechanical power pattern was likewise very similar to African elephants, showing spring-like power bursts associated with the hindlimbs at moderately fast speeds, unlike slow speeds (figure 12).

To quantify the transduction between potential and kinetic energies, we calculated the mechanical energy recovery (§2) for all elephants across their entire speed range (figure 13*a*). The associated phase shift angle between the potential and kinetic energies at different speeds is shown in figure 13*b*. The energy recovery reached its maximum of approximately 0.35–0.50 at a dimensionless speed ($Fr^{0.5}$) of 0.30. The corresponding phase angle was approximately 160° (140°–180°), i.e. the potential and kinetic energies were almost out of phase. With increasing speed, the energy recovery decreased gradually, associated with simultaneous decreases of phase angle. Interestingly, both energy recovery and phase shift angle appear to have levelled off after a dimensionless speed of approximately 0.50 (Fr 0.25), with values approaching energy recovery of 0.10 (0.06–0.15) and phase angle of 90° (70°–110°). When the speed was slower than normal, both energy recovery and phase angle decreased.

4. DISCUSSION

In this study, we have quantified the three-dimensional locomotor dynamics of African and Asian elephants using a novel multisensor method incorporating three-dimensional accelerometers and three-dimensional gyroscopes. Our methodology has some advantages over standard force platform analysis (also see Pfau *et al.* 2005, 2006): animal locomotion can be studied in open-field environments and across any ground surface; data collection is continuous (the sensors go where the animal goes) without being restricted to smaller plate areas; the equipment is reasonably inexpensive and requires little set-up time or maintenance, and runs on self-contained batteries; and three-dimensional body motion is measured allowing for internal work calculations. However, the technique involves errors (e.g. skin motion artefacts) and signal noises, only estimates rather than directly measures locomotor mechanics (e.g. ground reaction forces) and requires estimation of the CM position of the animal. But if caution is taken to deal with (and examine with sensitivity analysis) these errors and noises, this kinematics-based method can still produce good results compared with methods based on force transducers (e.g. force plates). For example, Bobbert *et al.* (1991) used a very simple motion analysis marker system, and successfully predicted the ground impact peak during human running with less than 10% error compared with force plate data. Ladin & Wu (1991) successfully estimated the forces exerted on a pivot joint using only one triaxial accelerometer. The results matched well with the measured forces using an instrumented array of strain gauges in the pivot joint. Van den Bogert *et al.* (1996) found that four triaxial accelerometers attached on the torso reasonably reproduced the patterns of force plate data for human walking and running. Bobbert *et al.*

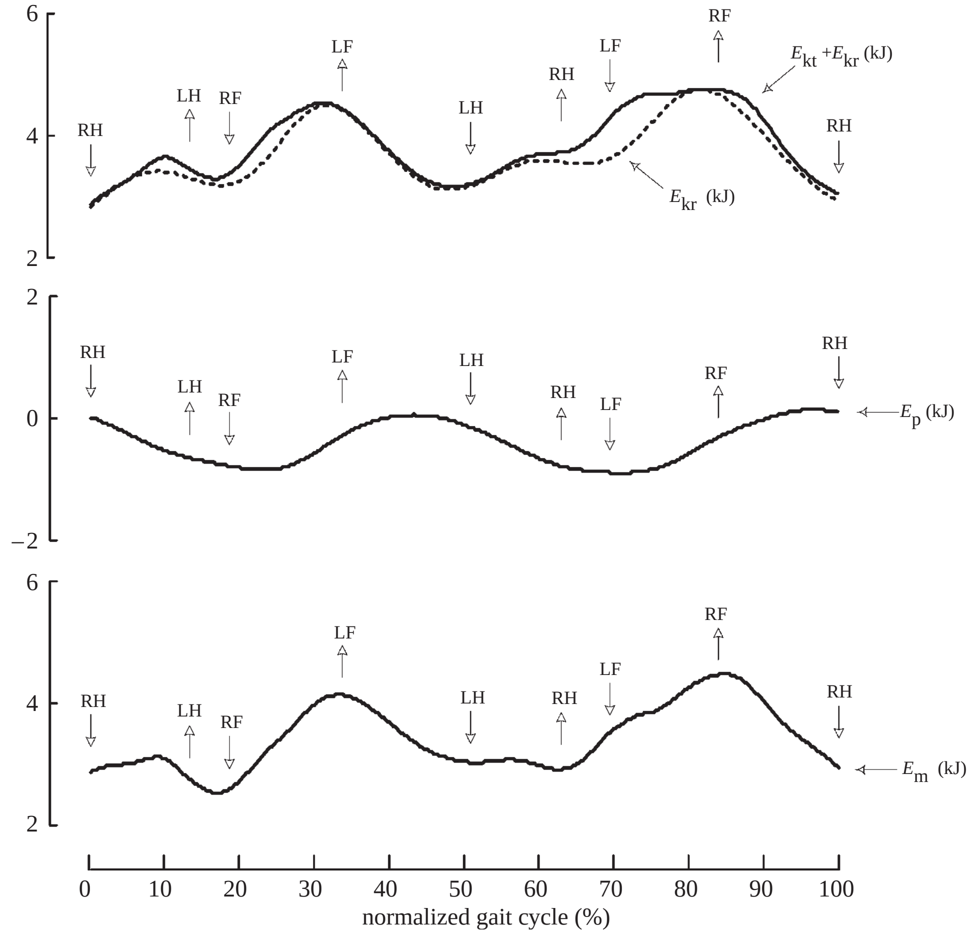

Figure 10. Representative time histories of translational kinetic energy $E_{\rm kt}$, total kinetic energy $E_{\rm kt}+E_{\rm kr}$, potential energy $E_{\rm p}$ and total mechanical energy $E_{\rm m}$ in a stride cycle of an Asian elephant (3000 kg) moving at 1.56 m s^{-1} (Fr 0.12), averaged for three continuous strides (cf. figure 7).

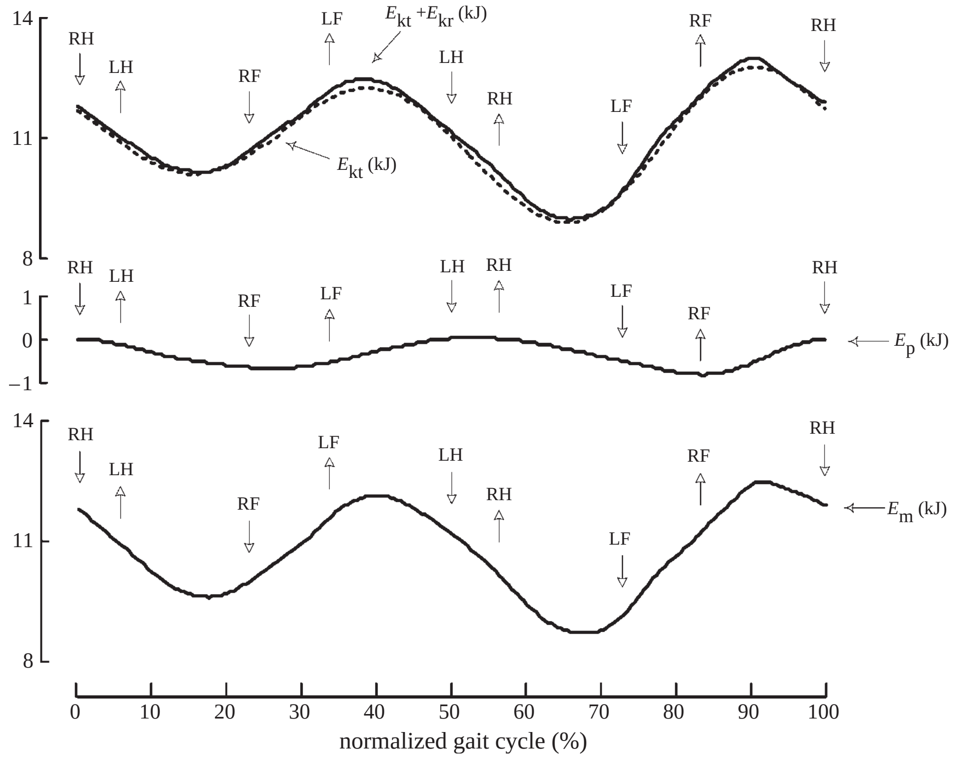

Figure 11. Representative time histories of translational kinetic energy $E_{\rm kt}$, total kinetic energy $E_{\rm kt}+E_{\rm kr}$, potential energy $E_{\rm p}$ and total mechanical energy $E_{\rm m}$ in a stride cycle of an Asian elephant (3000 kg) moving at 2.41 m s^{-1} (Fr 0.30), averaged for two continuous strides (cf. figure 8).

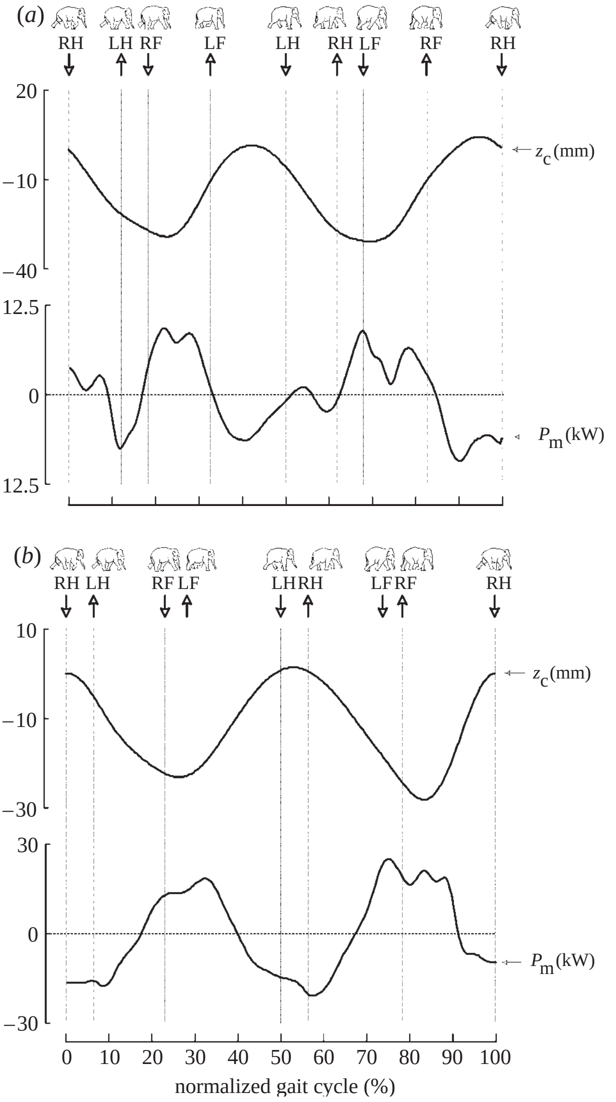

Figure 12. Representative averaged time histories of vertical CM displacement and total mechanical power in a stride cycle of an Asian elephant (3000 kg) moving at (*a*) 1.56 m s^{-1} (Fr 0.12) and (*b*) 2.41 m s^{-1} (Fr 0.30) (cf. figure 9). Elephant pictures modified from Gambaryan (1974).

(2007) successfully calculated the vertical ground reaction forces on individual limbs of horses based only on some marker kinematics data. The estimated forces concurred with the measured force plate data.

The current method does not directly account for the motions of the limbs and head, although our three-dimensional CM model (figure 4) included these appendages. However, the ratios of elephant's limb and head/neck masses to the whole body mass are moderate; overall they are close to those of horses (6–9% of body mass per limb for horses and elephants; 9.5% body mass for head/neck for horses, approx. 15% for elephants; Shoshani *et al.* 1982; Buchner *et al.* 1997; also supported by our three-dimensional CM model's data). In addition, as the elephant's touchdown and lift-off angles are small, and change only slightly with increasing speed (our unpublished limb motion data (2006)), the effect of limb motion on CM estimation would be small. Additionally, according to our observations based on video data (e.g. Hutchinson *et al.* 2006), the motions of the head and forequarters largely

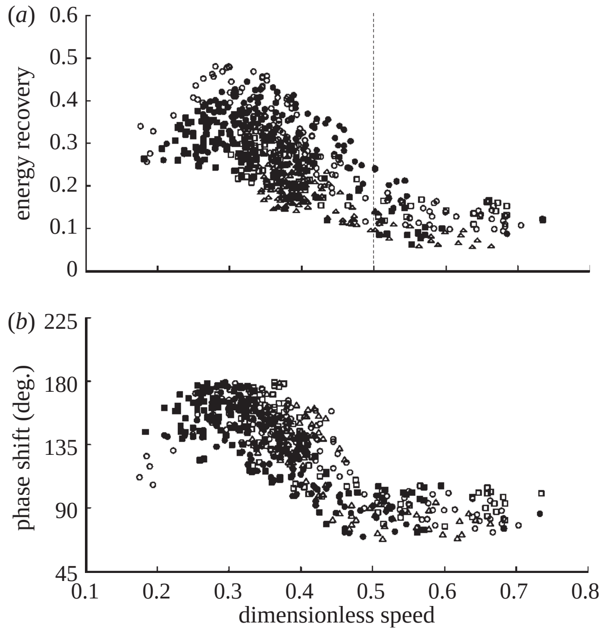

Figure 13. (*a*) Mechanical energy recovery and (*b*) phase shift angle between potential energy and kinetic energies plotted against dimensionless speed (Fr$^{0.5}$) for African (open symbols) and Asian (filled symbols) elephants.

move out of phase, which may cancel each other's motions out to some extent. Hence, we are confident that the errors induced by neglecting the head and limb motions in our method will be small (see also van den Bogert *et al.* 1996; Pfau *et al.* 2005, 2006) and should not change the major trends. These assumptions are validated by using multi-segment kinematic data (see electronic supplementary material).

Our results show that, like stride parameters (Hutchinson *et al.* 2006), the CM motions of African and Asian elephants are qualitatively quite similar. The body CM of both species reached its highest position around forelimb mid-stance with small fluctuation amplitudes (around 3 cm), and increased slightly with increasing speed. This vertical CM displacement was of very small amplitude; however, it is consistent with our previous kinematic data. The peak vertical displacement of the hip and shoulder skin markers at any speed is very small (generally less than 0.10 m, often less than 0.05 m; Hutchinson *et al.* 2006). As these displacements are out of phase to some extent even at moderately fast speed (Hutchinson *et al.* 2003, 2006), this may further flatten the CM vertical displacement pattern. Gambaryan (1974) reached comparable conclusions independently, inferring a rather horizontal CM path. Furthermore, this fluctuation amplitude is comparable to that of tölting horses (Biknevicius *et al.* 2006) based on force plate data, which is approximately 1.2 cm (less than 1% of limb length, even lower than the approx. 1.5% of hip height relative peak displacement values in our elephants). However, our inertial sensor processing may slightly reduce the CM displacement, as the digital filtering process (see §2) will remove some signals when reducing the noise (Winter 1990). Yet this is inevitable for all motion analysis methods even the multiple camera system (Winter 1990; Pfau *et al.* 2005) as the noises, e.g. skin movements, are in a similar frequency band as the useful motion signals. As we have chosen a well-validated and publicly recognized digital filtering method (Winter *et al.* 1974; Winter 1990), this reduction should be minimized.

Like kinematic patterns, the kinetics of African and Asian elephants are also quite similar. The body CM kinetic and potential energies of both species of elephants have out-of-phase relationships at their energetically optimal speed around a dimensionless (relative) speed of 0.30 (Fr 0.09, approx. 1.3 m s^{-1}; figures 7 and 10), as mechanical energy recovery reaches its maximum (figure 13*a*). This coincides with the observation that elephants' metabolic cost of transport (J $kg^{-1}m^{-1}$) is minimal at their normal moving speed (Langman *et al.* 1995), consistent with the inference that they may use a passive inverted pendulum (and perhaps some elastic; Geyer *et al.* 2006) mechanism(s) to conserve energy at their optimal speed, like most other terrestrial animals (Cavagna *et al.* 1977; Blickhan & Full 1993; Farley & Ko 1997; Ahn *et al.* 2004; Rubenson *et al.* 2004; Biewener 2006; Biknevicius & Reilly 2006). Their maximal energy recovery may appear to be lower than that of typical walking quadrupeds (approx. 60–75%; Cavagna *et al.* 1977; Griffin *et al.* 2004*a*; Usherwood *et al.* 2007), but this may be explained by their relatively smaller vertical CM displacement, which leads to small potential energy fluctuations. This will reduce the transduction between the potential and kinetic energies when they are out of phase, and hence result in small energy recovery. A similar pattern was observed in tölting horses (Biknevicius *et al.* 2006). Additionally, at normal moving speed (approx. Fr 0.10), the elephants' potential energy fluctuations reach their maxima between mid-stance of the supporting hindlimb and mid-stance of the supporting forelimb, which is very similar to the findings of previous studies of quadrupedal walking in which the limbs were modelled as rigid struts (Griffin *et al.* 2004*a*; Usherwood *et al.* 2007). This indicates that probably both the supporting forelimbs and the hindlimbs use vaulting mechanics during normal walking, as expected. However, in any case, we urge caution in overinterpreting our recovery values relative to other animals (or relative to energetic costs in elephants), as some errors inevitably are involved in our method, and along with other factors (including the assumptions of the recovery method itself) this renders comparison of recovery magnitudes among species far from straightforward.

At slower than normal speeds, the metabolic cost of transport increases (Langman *et al.* 1995) with decreasing mechanical energy recovery (figure 13*a*), which is consistent with previous force plate and modelling measurements of other quadrupeds (Cavagna *et al.* 1977; Griffin *et al.* 2004*a*; Usherwood *et al.* 2007). This may explain why elephants do not habitually move very slowly (indeed it is difficult to convince them to maintain very slow speeds), as their energy-conserving mechanisms may be less effective in this speed range.

At higher than normal speeds, the energy recovery decreased gradually (figure 13*a*), associated with simultaneous decreases of phase angle (figure 13*b*), suggesting less vaulting and increased bouncing mechanics for the limbs. Both energy recovery and phase shift angle levelled off after a dimensionless speed of approximately 0.50 (approx. 2.2 m s^{-1}); the patterns are strikingly reminiscent of a very different animal using a 'grounded run' (i.e. no whole-body aerial phase but bouncing mechanics): ostriches (Rubenson *et al.* 2004). Associated with the mechanical power patterns and the vertical CM displacements (figures 9 and 12), these data bolster the hypothesis that a gait transition may happen at this relatively slow speed. But were all or just some limbs using bouncing mechanics?

Our mechanical power analysis found that elephants use a spring-like power burst pattern at moderate speeds (greater than 2.2 m s^{-1}, Fr$\geqq$0.25), which is more associated with the hindlimbs. After hindlimb touchdown, as the contralateral shoulder joint is rolling down from its highest position, the hindlimb should generate a braking force as in a typical quadrupeds, absorbing mechanical energies in early stance phase, then presumably generating propulsive power, probably from middle to late stance, to push the body CM over the ipsilateral forelimb. After the contralateral forelimb left the ground, when only the ipsilateral forelimb and hindlimb were in stance, the forelimb should produce a braking force in its early stance (as in a typical quadruped); however, the total CM power was of large positive value at this time, which means that the stance hindlimb should have produced a larger propulsive power to counteract the braking forelimb and push the body CM. This indicates that the propulsion was probably contributed mainly by the hindlimbs. The whole-body CM displacement is more closely associated with the stance forelimb motion, reaching its maximum around forelimb mid-stance. As the elephant's body CM is closer to the forelimbs (Thompson 1917; Henderson 2006; this study), and the forelimbs remain very straight during the stance phase (Hutchinson *et al.* 2003, 2006), this indicates that the forelimbs most likely still use vaulting mechanics even at faster speeds. Although the vertical CM displacement showed a similar two-peaked pattern at both slower and faster speeds, its highest position moved towards the contralateral hindlimb touchdown as speed increased. As the forelimb remained fairly straight, this phase shift indicates that the hindlimb probably compressed at least during its early stance phase, as the CM vertical displacement of a bouncing hindlimb should peak at touchdown whereas a vaulting hindlimb should reach its highest position in its mid-stance. Therefore, a vaulting hindlimb would make the CM maximum vertical displacement point shift away from the contralateral hindlimb touchdown, which is contradictory to our data (figures 9 and 12).

Therefore, it is reasonable to hypothesize that when speed increased, the elephant's locomotor pattern changed smoothly from a fairly stiff-limbed vaulting gait to a more bouncing gait. Beyond a dimensionless speed of 0.50 (approx. 2.2 m s^{-1}), the hindlimbs exhibited some bouncing mechanics that we infer helped to push the elephant's body CM over their strut-like vaulting forelimbs. However, this mechanism differs from other quadrupedal bouncing gaits at medium speeds, e.g. trotting or pacing. The potential and kinetic energies were not exactly in phase, and there were still some interchanges between potential and kinetic energies, presumably related to the more straightened forelimbs (e.g. Hutchinson *et al.* 2006).

The mechanical energy analysis conducted in this study is mainly about the whole-body CM, rather than individual limbs. Our hypothesis of hindlimb-powered bouncing is mainly inferred from the whole-body CM dynamics and the footfall timings. The forelimbs are probably also involved to drive the body CM in addition to the hindlimb bouncing to some extent (which cannot be determined here), e.g. contralateral forelimb push-off around each hindlimb's mid-stance. Although some speculations are involved, this is the explanation that is most consistent with all available lines of evidence. Indeed, the rather slow speed gait transition revealed by this study concurs with previous results from kinematics: at moderately rapid speeds, the shoulder motion in stance phase still resembles walking, moving upwards and then downwards, whereas the hip motion is characteristic of running, moving downwards and then upwards (Hutchinson *et al.* 2003, 2006). Additionally, our conclusions are also consistent with stride parameter studies on African and Asian elephants. The regression slopes of stance phase duration, swing phase duration and relative stride length versus speed all show slight changes (discontinuities) before and after dimensionless speed 0.50 (greater than $2.2\ \mathrm{m\,s^{-1}}$, $\mathrm{Fr}>0.25$; Hutchinson *et al.* 2006).

In a classical kinematic sense, elephants do not run (Hildebrand 1985; Hutchinson *et al.* 2003, 2006). However, this does not mean that they do not use any bouncing mechanism (Hutchinson *et al.* 2003, 2006; also see Biewener 2006; Biknevicius & Reilly 2006). Our mechanical energy analysis suggests that elephants probably use a special locomotor pattern at moderate speeds (greater than $2.2\ \mathrm{m\,s^{-1}}$, $\mathrm{Fr}\geqq 0.25$), characterized by vaulting forelimb and probably bouncing hindlimb mechanics. These locomotor dynamics, combining vaulting and bouncing mechanics, are similar to those seen in cantering/galloping (Cavagna *et al.* 1977; Minetti 2000; Pfau *et al.* 2006) and 'intermediate gaits' (Ahn *et al.* 2004; Biknevicius & Reilly 2006).

The fastest speed recorded in this study for the captive elephants is $3.5\ \mathrm{m\,s^{-1}}$ ($\mathrm{Fr}\leq 0.56$), which is slower than the near-maximal speed of more athletic elephants ($6.8\ \mathrm{m\,s^{-1}}$, $\mathrm{Fr}\leq 3.4$). What happens when speed increases? Is there another gait transition as elephants approach their near-maximal speed? Previous studies on elephant stride parameters inferred that elephants must change their gait pattern by a dimensionless speed (or Fr) of 1.0 (Hutchinson *et al.* 2006). Near Fr 1.0, an elephant's forelimbs and hindlimbs attain their own separate aerial phases, so their fore and hindquarters could biomechanically be running. Those studies also found that at least the hindlimbs showed increasingly compliant motion. Although the forelimbs surely have some compliance, they still should be appreciably stiffer than the hindlimbs, as the shoulder joint retains its highest vertical position in forelimb mid-stance even at near-maximal speed (Hutchinson *et al.* 2003, 2006). However, we can only determine what the gait of fast moving elephants is when whole-body dynamics data at faster speeds are available.

Although athletic elephants can attain speeds over Fr 1.0 and as quick as Fr 3.4 (Hutchinson *et al.* 2003), we hypothesize that they change their locomotor pattern to a hindlimb bouncing gait at much slower, moderate speeds. This is surprisingly less than the medium gait transition speed of most other animals (e.g. from walking to running or trotting), which is usually Fr 0.4–0.6 (Alexander & Jayes 1983; Usherwood 2005). However, the elephant gait transition at $\mathrm{Fr}\sim 0.25$ is very close to the walk–trot gait transition speed (approx. 0.3; Alexander & Jayes 1983; J.R.H. 2006, unpublished data) of white rhinoceroses (*Ceratotherium simum*), the second largest land animals. Unlike elephants, rhinoceroses can trot and gallop (Alexander & Jayes 1983; Alexander & Pond 1992), which is typical of less graviportal quadrupeds. Furthermore, horses switch to trotting at slightly low Froude numbers as well (approx. 0.35; Griffin *et al.* 2004*b*), suggesting that this is a common pattern for larger quadrupedal mammals, although more data are needed to further test how broadly this trend applies. Why might large mammals change their gait at relatively slower speeds ($\mathrm{Fr}<0.40$)? We speculate that this may be because more compliant limb mechanics can attenuate transient impact forces on the feet (McMahon 1985; McMahon *et al.* 1987; Blickhan 1989), and hence reduce the risk of limb injury incurred by the massive body weight. In addition, bouncing limb mechanics helps to modulate vertical CM oscillations (Biknevicius *et al.* 2006; Schmitt *et al.* 2006), which may be particularly critical for the locomotor stability (and efficiency) of large quadrupeds.

The lateral sequence single-foot pattern used by elephants has been observed at slow walking speeds in a broad range of mammals (Muybridge 1899; Gambaryan 1974; Hildebrand 1985). But few species retain this footfall pattern into faster speeds, including elephants and horses (Hutchinson *et al.* 2003, 2006; Biknevicius *et al.* 2004, 2006; Schmitt *et al.* 2006). Some gaited horses, such as the Icelandic horse (tölt) and the Paso Fino horse (classic fino, paso largo), can move quite rapidly using the single footfall pattern without changing to trotting or galloping (Biknevicius *et al.* 2004, 2006), which is very similar to the kinematics of elephants. However, in a biomechanical sense, the tölt of Icelandic horses is a running (i.e. bouncing) gait (Biknevicius *et al.* 2006). Tölting Icelandic horses have an almost in-phase kinetic and potential energy relationship with a phase shift angle much less than 90° (often less than 45°), and the body CM is at its lowest position during the forelimb mid-stance (Biknevicius *et al.* 2006). These are all typical features of a purely running gait. It remains to be seen whether past $\mathrm{Fr}\sim 1.0$ elephants move in this fashion.

Elephants at moderate speed move rather unlike tölting in that they seem to have a combined vaulting and bouncing gait. Although the quadrupedal walking of many mammals is to some extent driven by the hindlimbs (Manter 1938; Demes *et al.* 1994; Gregersen *et al.* 1998), we infer that elephants feature extreme specialization of the forelimbs as stiff supportive struts, whereas the hindlimbs act as bouncing motors. This mechanism may provide biomechanical advantages for the largest land animals during natural locomotion. The bouncing of the stance limbs may provide some energetic benefits for these animals by reducing muscular work when they move fast, similar to the energy-saving mechanisms found in other bouncing gaits (Alexander 1988, 1991; Farley *et al.* 1993). However, a more crouched, bouncing hindlimb should cause a reduced effective mechanical advantage of extensor muscles and a consequent increase of muscle force production, which could be a trade-off for this elastic energy-saving mechanism (Biewener *et al.* 2004). Furthermore, the evenly spaced single-foot pattern (Hildebrand 1976, 1985; Hutchinson *et al.* 2006) provides superior stability at faster speeds because the supporting base is normally larger and the simultaneous counteractions of forelimb and hindlimb throughout the stride help to preserve body stability along the direction of progression (Manter 1938; Hildebrand 1976, 1985; Winter 1990; Donelan *et al.* 2002). Thus, at medium speeds elephants may take advantage of both spring mass and inverted pendulum mechanisms while retaining superior body stability typically only associated with slower gaits.

Finally, our analysis defies the classic dogma that elephants do not run in any sense because they are either too large or have overly rigid, inflexible limbs that prevent bouncing (Alexander & Pond 1992; Paul 1998). It is conceivable that other parts of elephants (e.g. the head or internal organs) contribute some bouncing, but our data support the hypothesis that at least the hindlimbs bounce at moderate-to-high speeds. As Gambaryan (1974) also noted, elephants have extraordinarily rigid bodies; hence, we expect that our assumption that the body is effectively rigid is more justifiable for them than for most other animals. The second gait of elephants could be called an amble, intermediate gait or run (Muybridge 1899; Gambaryan 1974; Alexander *et al.* 1979; Ahn *et al.* 2004; Schmitt *et al.* 2006), and raises the question of whether gaits may be better defined by individual limb dynamics (e.g. vaulting or bouncing of particular limbs) rather than whole-body CM dynamics (Biewener 2006; Biknevicius & Reilly 2006). However, we caution that the kinematic (Hutchinson *et al.* 2003, 2006) and kinetic (this study; especially figure 13) changes as elephants increase in speed are fairly continuous, perhaps involving a more gradual and subtle gait transition that blurs the distinction between seemingly discrete gaits (also see Ruina *et al.* 2005; Geyer *et al.* 2006). Although this strays dangerously into semantic issues, the shift from vaulting to bouncing hindlimb mechanics we have inferred from slow to fast speeds in elephants is a major change of locomotor function that was not suspected or as thoroughly demonstrated in previous studies, and hence we view it as a distinct gait. We expect that other aspects of prevailing locomotor paradigms about large 'graviportal' mammals and the biomechanical constraints that large size imposes on locomotor capabilities will need further revision as additional empirical data on their locomotor mechanics become available.

All experiments with elephants were conducted with the approval of the Royal Veterinary College's Ethics and Welfare Committee.

We thank the elephant handlers and other facilitators at Woburn Safari Park (Lynne Thomson and staff) and West Midlands Safari Park (Andy Plumb, Becky Wardle and staff) for their patience in making our experiments not only feasible but also safe, efficient and enjoyable. Charlotte Miller, Karin Jespers and other members of the Structure and Motion Laboratory gave hands-on assistance. Victor Ng-Thow-Hing developed the three-dimensional modelling software and Mark Burgess created the three-dimensional elephant model. Vivian Allen contributed to analysing the three-dimensional elephant model. We also thank Charlotte Miller, Kevin Parsons, Thilo Pfau, Jim Usherwood and Alan Wilson and five anonymous reviewers for their input that improved this study. Funding for this research was provided in 2005 by the BBSRC for New Investigator grant number BB/C516844/1.

REFERENCES

Ahn, A. N., Furrow, E. & Biewener, A. A. 2004 Walking and running in the red-legged running frog, *Kassina maculata*. *J. Exp. Biol.* **207**, 399–410. (doi:10.1242/jeb.00761)

Alexander, R. McN. 1977 Allometry of the limbs of antelopes (Bovidae). *J. Zool.* **183**, 125–146.

Alexander, R. McN. 1988 *Elastic mechanisms in animal movement*. Cambridge, UK: Cambridge University Press.

Alexander, R. McN. 1991 Energy-saving mechanism in walking and running. *J. Exp. Biol.* **160**, 55–69.

Alexander, R. McN. & Jayes, A. S. 1983 A dynamic similarity hypothesis for the gaits of quadrupedal mammals. *J. Zool.* **201**, 135–152.

Alexander, R. McN. & Pond, C. M. 1992 Locomotion and bone strength of the White Rhinoceros, *Ceratotherium simum*. *J. Zool.* **227**, 63–69.

Alexander, R. McN., Maloiy, G. M. O., Hunter, B., Jayes, A. S. & Nturibi, J. 1979 Mechanical stresses in fast locomotion of buffalo (*Syncerus caffer*) and elephant (*Loxodonta africana*). *J. Zool. Lond.* **189**, 135–144.

Biewener, A. A. 2006 Patterns of mechanical energy change in tetrapod gait: pendula, spring and work. *J. Exp. Zool. A* **305**, 899–911. (doi:10.1002/jez.a.334)

Biewener, A. A. & Taylor, C. R. 1986 Bone strain: a determinant of gait and speed? *J. Exp. Biol.* **123**, 383–400.

Biewener, A. A., Farley, C. T., Roberts, T. J. & Temaner, M. 2004 Muscle mechanical advantage of human walking and running: implications for energy cost. *J. Appl. Physiol.* **97**, 2266–2274. (doi:10.1152/japplphysiol.00003.2004)

Biknevicius, A. R. & Reilly, S. M. 2006 Correlation of symmetrical gaits and whole body mechanics: debunking myths in locomotor biodynamics. *J. Exp. Zool. A* **305**, 923–934. (doi:10.1002/jez.a.332)

Biknevicius, A. R., Mullineaux, D. R. & Clayton, H. M. 2004 Ground reaction forces and limb function in tölting horses. *Equine Vet. J.* **36**, 743–747. (doi:10.2746/0425164044848190)

Biknevicius, A. R., Mullineaux, D. R. & Clayton, H. M. 2006 Locomotor mechanics of the tölt in Icelandic horses. *Am. J. Vet. Res.* **67**, 1505–1510. (doi:10.2460/ajvr.67.9.1505)

Blickhan, R. 1989 The spring-mass model for running and hopping. *J. Biomech.* **22**, 1217–1227. (doi:10.1016/0021-9290(89)90224-8)

Blickhan, R. & Full, R. J. 1993 Mechanical work in terrestrial locomotion. In *Structures and systems* (ed. A. A. Biewener), pp. 75–96. New York, NY: Oxford University Press.

Bobbert, M. F., Schamhardt, H. C. & Nigg, B. M. 1991 Calculation of vertical ground reaction force estimates during running from position data. *J. Biomech.* **24**, 1095–1105. (doi:10.1016/0021-9290(91)90002-5)

Bobbert, M. F., Gómez Álvarez, C. B., van Weeren, P. R., Roepstorff, L. & Weishaupt, M. A. 2007 Validation of vertical ground reaction forces on individual limbs calculated from kinematics of horse locomotion. *J. Exp. Biol.* **210**, 1885–1896. (doi:10.1242/jeb.02774)

Buchner, H. H. F., Savelberg, H. H. C. M., Schamhardt, H. C. & Barneveld, A. 1997 Inertial properties of Dutch warmblood horses. *J. Biomech.* **30**, 653–658. (doi:10.1016/S0021-9290(97)00005-5)

Campbell, S. L. & Meyer Jr, C. D. 1991 *Generalized inverses of linear transformations.* New York, NY: Dover.

Cavagna, G. A. & Kaneko, M. 1977 Mechanical work and efficiency in level walking and running. *J. Physiol.* **268**, 467–481.

Cavagna, G. A., Heglund, N. C. & Taylor, C. R. 1977 Mechanical work in terrestrial locomotion: two basic mechanisms for minimizing energy expenditure. *Am. J. Physiol.* **233**, R243–R261.

Christiansen, P. 2004 Body size in proboscideans, with notes on elephant metabolism. *Zool. J. Linn. Soc.* **140**, 523–549. (doi:10.1111/j.1096-3642.2004.00113.x)

Coombs, W. P. 1978 Theoretical aspects of cursorial adaptations in dinosaurs. *Q. Rev. Biol.* **53**, 393–415. (doi:10.1086/410790)

Demes, B., Larson, S. G., Stern Jr, J. T., Jungers, W. L., Biknevicius, A. R. & Schmitt, D. 1994 The kinetics of primate quadrupedalism: hindlimb drive. *J. Hum. Evol.* **26**, 353–374. (doi:10.1006/jhev.1994.1023)

Donelan, J. M., Kram, R. & Kuo, A. D. 2002 Simultaneous positive and negative external mechanical work in human walking. *J. Biomech.* **35**, 117–124. (doi:10.1016/S0021-9290(01)00169-5)

Farley, C. T. & Ko, T. C. 1997 Mechanics of locomotion in lizards. *J. Exp. Biol.* **200**, 2177–2188.

Farley, C. T. & Taylor, C. R. 1991 A mechanical trigger for the trot-gallop transition in horses. *Science* **253**, 306–308. (doi:10.1126/science.1857965)

Farley, C. T., Glasheen, J. & McMahon, T. A. 1993 Running springs: speed and animal size. *J. Exp. Biol.* **185**, 71–86.

Gambaryan, P. P. 1974 *How mammals run.* New York, NY: Wiley.

Geyer, H., Seyfarth, A. & Blickhan, R. 2006 Compliant leg behaviour explains basic dynamics of walking and running. *Proc. R. Soc. B* **273**, 2861–2867. (doi:10.1098/rspb.2006.3637)

Gray, J. 1968 *Animal locomotion.* New York, NY: W. W. Norton & Co., Inc.

Gregersen, C. S., Silverton, N. A. & Carrier, D. R. 1998 External work and potential for elastic storage at the limb joints of running dogs. *J. Exp. Biol.* **201**, 3197–3210.

Gregory, W. K. 1912 Notes on the principles of quadrupedal locomotion and the mechanisms of the limbs in hoofed animals. *Ann. NY Acad. Sci.* **22**, 267–292. (doi:10.1111/j.1749-6632.1912.tb55164.x)

Griffin, T. M., Main, R. P. & Farley, C. T. 2004*a* Biomechanics of quadrupedal walking: how do four-legged animals achieve pendulum-like mechanics? *J. Exp. Biol.* **207**, 3545–3558. (doi:10.1242/jeb.01177)

Griffin, T. M., Kram, R., Wickler, S. J. & Hoyt, D. F. 2004*b* Biomechanical and energetic determinants of the walk–trot transition in horses. *J. Exp. Biol.* **207**, 4215–4223. (doi:10.1242/jeb.01277)

Hayes, W. C., Gran, J. D., Nagurka, M. L., Feldman, J. M. & Oatis, C. 1983 Leg motion analysis during gait by multiaxial accelerometry; theoretical foundations and preliminary validations. *J. Biomech. Eng.* **105**, 283–289.

Heglund, N. C., Cavagna, G. A. & Taylor, C. R. 1982*a* Energetics and mechanics of terrestrial locomotion III: energy changes of the centre of mass as a function of speed and body size in birds and mammals. *J. Exp. Biol.* **97**, 41–56.

Heglund, N. C., Cavagna, G. A. & Taylor, C. R. 1982*b* Energetics and mechanics of terrestrial locomotion IV: total energy changes as a function of speed and body size in birds and mammals. *J. Exp. Biol.* **97**, 57–66.

Henderson, D. M. 2006 Burly gaits: centers of mass, stability, and the trackways of sauropod dinosaurs. *J. Vert. Paleontol.* **26**, 907–921. (doi:10.1671/0272-4634(2006)26[907:BGCOMS]2.0.CO;2)

Hildebrand, M. 1976 Analysis of tetrapod gaits: general considerations and symmetrical gaits. In *Neural control of locomotion* (eds P. S. G. Stein & D. G. Smart), pp. 203–236. New York, NY: Plenum Press.

Hildebrand, M. 1985 Walking and running. In *Functional vertebrate morphology* (eds M. Hildebrand, D. M. Bramble & K. F. Liem), pp. 38–57. Cambridge, MA: Harvard University Press.

Hoyt, D. F. & Taylor, C. R. 1981 Gait and the energetics of locomotion in horses. *Nature* **292**, 239–240. (doi:10.1038/292239a0)

Hutchinson, J. R., Famini, D., Lair, R. & Kram, R. 2003 Biomechanics: are fast-moving elephants really running? *Nature* **422**, 493–494. (doi:10.1038/422493a)

Hutchinson, J. R., Schwerda, D., Famini, D., Dale, R. H. I., Fischer, M. & Kram, R. 2006 The locomotor kinematics of African and Asian elephants: changes with speed and size. *J. Exp. Biol.* **209**, 3812–3827. (doi:10.1242/jeb.02443)

Hutchinson, J. R., Ng-Thow-Hing, V. & Anderson, F. C. 2007 A 3D interactive method for estimating body segmental parameters in animals: application to the turning and running performance of *Tyrannosaurus rex*. *J. Theor. Biol.* **246**, 660–680. (doi:10.1016/j.jtbi.2007.01.023)

Kane, T. R., Hayes, W. C. & Priest, J. D. 1974 Experimental determination of forces exerted in tennis play. In *Biomechanics IV* (eds R. C. Nelson & C. A. Morehouse), pp. 284–290. Baltimore, MD: University Park Press.

Kuo, A. D. 2002 Energetics of actively powered locomotion using the simplest walking model. *J. Biomech. Eng.* **124**, 113–120. (doi:10.1115/1.1427703)

Ladin, Z. & Wu, G. 1991 Combining position and acceleration measurements for joint force estimation. *J. Biomech.* **24**, 1173–1187. (doi:10.1016/0021-9290(91)90009-C)

Langman, V. A., Roberts, T. J., Black, J., Maloiy, G. M. O., Heglund, N. C., Weber, J.-M., Kram, R. & Taylor, C. R. 1995 Moving cheaply: energetics of walking in the African Elephant. *J. Exp. Biol.* **198**, 629–632.

Manter, J. T. 1938 The dynamics of quadrupedal walking. *J. Exp. Biol.* **15**, 522–540.

McGeer, T. 1992 Principles of walking and running. In *Advances in comparative and environmental physiology: mechanics of animal locomotion* (ed. R. McN. Alexander), pp. 133–139. Berlin, Germany: Springer.

McMahon, T. A. 1985 The role of compliance in mammalian running gaits. *J. Exp. Biol.* **115**, 263–282.

McMahon, T. A., Valiant, G. & Frederick, E. C. 1987 Groucho running. *J. Appl. Physiol.* **62**, 2326–2337.

Morris, J. R. W. 1973 Accelerometry—a technique for the measurement of human body movements. *J. Biomech.* **6**, 729–732. (doi:10.1016/0021-9290(73)90029-8)

Muybridge, E. 1899 *Animals in motion.* New York, NY: Dover.

Minetti, A. E. 2000 The three modes of terrestrial locomotion. In *Biomechanics and biology of movement* (eds B. M. Nigg, B. R. MacIntosh & J. Mester), pp. 67–78. Champaign, IL: Human Kinetics.

Parsons, K. J. & Wilson, A. M. 2006 The use of MP3 recorders to log data from equine hoof mounted accelerometers. *Equine Vet. J.* **38**, 675–680. (doi:10.2746/042516406X156578)

Paul, G. S. 1998 Limb design, function and running performance in ostrich mimics and tyrannosaurs. *Gaia* **15**, 257–270.

Pfau, T., Witte, T. H. & Wilson, A. M. 2005 A method for deriving displacement data during cyclical movement using an inertial sensor. *J. Exp. Biol.* **208**, 2503–2514. (doi:10.1242/jeb.01658)

Pfau, T., Witte, T. H. & Wilson, A. M. 2006 Centre of mass movement and mechanical energy fluctuation during gallop locomotion in the thoroughbred racehorse. *J. Exp. Biol.* **209**, 3742–3757. (doi:10.1242/jeb.02439)

Rubenson, J., Heliams, D. B., Lloyd, D. G. & Fournier, P. A. 2004 Gait selection in the ostrich: mechanical and metabolic characteristics of walking and running with and without an aerial phase. *Proc. R. Soc. B* **271**, 1091–1099. (doi:10.1098/rspb.2004.2702)

Rubin, C. T. & Lanyon, L. E. 1984 Dynamic strain similarity in vertebrates; an alternative to allometric limb bone scaling. *J. Theor. Biol.* **107**, 321–327.

Ruina, A., Bertram, J. E. & Srinivasan, M. 2005 A collisional model of the energetic cost of support work qualitatively explains leg sequencing in walking and galloping, pseudo-elastic leg behavior in running and the walk-to-run transition. *J. Theor. Biol.* **14**, 170–192. (doi:10.1016/j.jtbi.2005.04.004)

Schmitt, D., Cartmill1, M., Griffin, T. M., Hanna, J. B. & Lemelin, P. 2006 Adaptive value of ambling gaits in primates and other mammals. *J. Exp. Biol.* **209**, 2042–2049. (doi:10.1242/jeb.02235)

Shoshani, J. *et al.* 1982 On the dissection of a female Asian elephant (*Elephas maximus maximus* Linneaus 1758) and data from other elephants. *Elephant* **2**, 3–93.

Thompson, D. W. 1917 *On growth and form.* Cambridge, UK: Cambridge University Press.

van den Bogert, A. J., Read, L. & Nigg, B. M. 1996 A method for inverse dynamic analysis using accelerometry. *J. Biomech.* **29**, 949–954. (doi:10.1016/0021-9290(95)00155-7)

Usherwood, J. R. 2005 Why not walk faster? *Biol. Lett.* **1**, 338–341. (doi:10.1098/rsbl.2005.0312)

Usherwood, J. R., Williams, S. B. & Wilson, A. M. 2007 Mechanics of dog walking compared with a passive, stiff-limbed, 4-bar linkage model, and their collisional implications. *J. Exp. Biol.* **210**, 533–540. (doi:10.1242/jeb.02647)

Winter, D. A. 1990 *The biomechanics and motor control of human movement*, 2nd edn. New York, NY: Wiley.

Winter, D. A., Sidwall, H. G. & Hobson, D. A. 1974 Measurement and reduction of noise in kinematics of locomotion. *J. Biomech.* **7**, 157–159. (doi:10.1016/0021-9290(74)90056-6)

Witte, T. H., Knill, K. & Wilson, A. M. 2004 Determination of peak vertical ground reaction force from duty factor in the horse (*Equus caballus*). *J. Exp. Biol.* **207**, 3639–3648. (doi:10.1242/jeb.01182)

Wood, G. L. 1972 *Animal facts and feats.* New York, NY: Doubleday & Company, Inc.